

HF Absorption and Static Electromagnetic Properties of NiCuZn Ferrites

CHING-CHIEN HUANG, YUNG-HSIUNG HUNG, JEN-YUNG HSU
and MING-FENG KUO

*New Materials Research & Development Department
China Steel Corporation*

Using a new and simple blade casting method, sintered NiCuZn ferrite electromagnetic wave absorber sheets, with lighter, thinner and high absorption properties, were first demonstrated. The electromagnetic wave absorption ability was enhanced by sintered NiCuZn ferrite absorbent. The experimental results reveal that NiCuZn ferrite absorber sheets with a thickness 0.1mm have the maximum reflection loss value above 0.74 dB at 11.26 MHz. A corresponding bandwidth of the reflection loss value above 0.3 dB and larger than 1.3 MHz is profitable for wideband electromagnetic wave absorption. The absorption properties could be controlled by the variation of the sintering temperature of the NiCuZn ferrite. A more homogenous microstructure revealed by SEM micrograph and a better crystalline XRD pattern may be responsible for the best absorption ability at 1150°C sintering temperature. The absorption properties were also successfully analyzed in this work, which took into account both the frequency at the reflection loss minimum f_r shift correlated with the value of inductance (L) and impedance (Z) of sintered toroidal cores and the power reflection loss (Γ) depending on ϵ'' , μ'' and $(\epsilon \times \mu)^{1/2}$, where ϵ and μ are complex relative dielectric permittivity and permeability, respectively, for the attenuation material. The sintered NiCuZn ferrite could be a potential candidate as an electromagnetic attenuation material to meet the demand for miniaturization, broader relative bandwidths at HF (3–30 MHz), and beneficial for the fabrication of radio frequency identification (RFID) metal tags.

Keywords: HF, Sinter, NiCuZn Ferrite, Absorber Sheet, RFID

1. INTRODUCTION

Sintered NiCuZn ferrites was first demonstrated as an electromagnetic wave absorber sheet in HF (3~30 MHz) region. Recently, RFID components have become a blossoming communication technique based on high frequency electromagnetic waves and have been used for logistics management. However, poor coupling between tags and readers could be caused by the destructive interference induced by a conductive atmosphere. The electromagnetic absorber sheet can improve the cross talk of RFID tags with their readers in the equipment, and the miniaturization of this component would permit a higher mounting density in equipment, enabling the fabrication of smaller, lighter and more functional electronic products.

Ferrite sheets are also a promising material for absorbing undesired electromagnetic waves generated by nearby equipment to avoid the electromagnetic interference (EMI) problem. The performance of the electromagnetic wave absorber sheet of ferrite is greatly affected by its electromagnetic properties. The minimal reflection of the microwave power or match-

ing condition occurs when the thickness of the absorber sheets approximates an odd number multiple of a quarter of the propagating wavelength. This phenomenon is due to the cancellation of the incidental and reflected waves at the surface of the absorber sheets. The electromagnetic absorbing properties of a sintering ferrite absorber sheet, including the plate thickness and the frequency at the reflection loss minimum (f_r), are determined by its dielectric constant (ϵ) and magnetic permeability (μ)⁽¹⁻³⁾. These electromagnetic properties are all controlled by the material composition, the particle size, and the content of the magnetic absorber sheet^(3,4). The properties of electromagnetic absorber sheets in sintered ferrite have been observed in some previous literatures, but systematic research between toroidal cores and sheets has not been carried out yet. NiCuZn ferrites are potential materials for HF application due to their high resistivity, high permeability, broad bandwidth, and low price⁽⁵⁾. In this article, the high absorption property of the HF absorber sheet is demonstrated. The correlation between sintered NiCuZn ferrite configurations of toroidal core and sheet were also addressed. A more detailed study was

also carried out to investigate the influences on the electromagnetic wave absorbing properties of sintering temperature, grain size and Ni content in NiCuZn ferrites. For a control of magnetic permeability, the effect of variations of Nicole content in NiCuZn ferrite was examined. Appropriate sintering conditions and chemical composition produced the thinner, lighter, and higher absorption properties required for absorber sheet used in the HF region.

2. EXPERIMENTAL METHOD

The chemical reagent powders of Fe_2O_3 , NiO, ZnO, and CuO were weighed and wet mixed in an attritor mill at the weight percentage (wt%) of $\text{Fe}_2\text{O}_3/\text{NiO}/\text{ZnO} / \text{CuO} = 65/6-14/15-20/4-7$, respectively, as shown in Table 1. Several additives such as CoO for grain resistance improvement and Bi_2O_3 , MoO_3 for grain growth are added to the mixtures. After being pulverizing by the attritor mill, the mixtures are then calcined for 1 hr at 900°C to prepare the magnetic absorbent. The absorber filler is composed of 95 wt% calcined magnetic absorbent, 5 wt% polyvinyl alcohol (PVA), and butanol. PVA is used as a binding agent and butanol as a dispersant. They will both evaporate after sintering. Absorber filler is subsequently filled into a $9\text{cm}\times 4\text{cm}\times 0.1\text{mm}$ mold shown in Fig.1(a) and then smoothed into a thin film by the blade casting method to form an absorber sheet as shown in Fig.1(b). The mold size can be modulated to manufacture the desired absorber sheet.

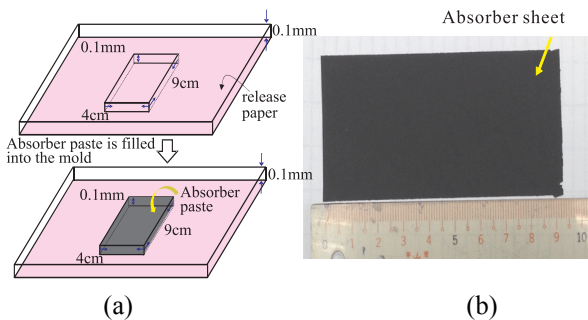


Fig.1. (a) Absorber filler is filled into $9\text{cm}\times 4\text{cm}\times 0.1\text{mm}$ mold; (b) The picture of absorber sheet.

After the absorber sheet had dried, it was removed from the mold and placed on a ZrO_2 substrate. Then the absorber sheet was sintered at $1050\sim 1200^\circ\text{C}$ for 1hr in air atmosphere to form the spinel ferrite. These kind of sintering ferrite absorber sheets are called ‘hard absorber sheets’ to distinguish them from the ferrite composite absorber sheets without sintering (i.e., soft absorber sheets). To investigate the effect of sintering temperature on the electromagnetic absorbing materials, sample C was chosen to be examined in this work. The phase of the sintered spinel ferrite was analyzed by X-ray diffraction. The grain size and shape were observed by scanning electron microscope. In order to compare the hard absorber sheet with the previous soft absorber sheet, we also prepared two kinds of soft absorber sheet (thickness = 0.1mm) using the technique developed by our group⁽¹⁾. The magnetic absorbents (A and B) used for the soft absorber sheets are also shown in Table 1.

The electromagnetic wave absorption ability was investigated by the measurement technique developed by our group⁽⁶⁾ using the absorber sheet as a substrate for the RFID tag to evaluate its ability to suppress destructive interference by measuring reflection loss⁽⁶⁾. An HF tag was first attached to the absorber sheet for the test and then placed on a metal plate surface. An RFID tag comprising a coil with a diameter of 2.5 cm and a capacitor was used in the present work, with the measurement setup being illustrated in Fig.2. In the system, a network analyzer (Agilent E5071B) was used to generate energy and simultaneously monitor the matching condition of the LC circuit from the power reflection loss (Γ) using a testing coil; the power reflection loss (Γ) is measured in decibels (dB). When a sintered absorber sheet is inserted between the tag and the metal plate, the magnetic field radiated from the tag is unimpacted by the metal plate and the RFID tag could work with the reader. The diminishment in Γ indicates the occurrence of absorption or the minimal reflection of the electromagnetic wave power. The diminishment suggests that a larger portion of energy emitted from the readers was consumed by RFID tag, and hence mutual

Table 1 Chemical composition of Soft/Hard absorber sheet

Composition (wt%)	Fe	Ni	Mo		f_r (MHz)	S_{11} (dB)				
Soft ⁽¹⁾	A	100	0	0	15.2	0.1				
	B	17	81	2	14.5	0.2				
Composition (wt%)	Fe_3O_4	ZnO	NiO	CuO	CoO	Bi_2O_3	MoO_3	f_r (MHz)	S_{11} (dB)	
Hard ⁽²⁾	C	65	20	9.4	4.1	0.5	0.06	0.06	11.26	0.74

⁽¹⁾ Soft absorber sheet: ferrite composite absorber sheet (thickness = 0.1mm).

⁽²⁾ Hard absorber sheet: sintering ferrite absorber sheet (thickness = 0.1mm).

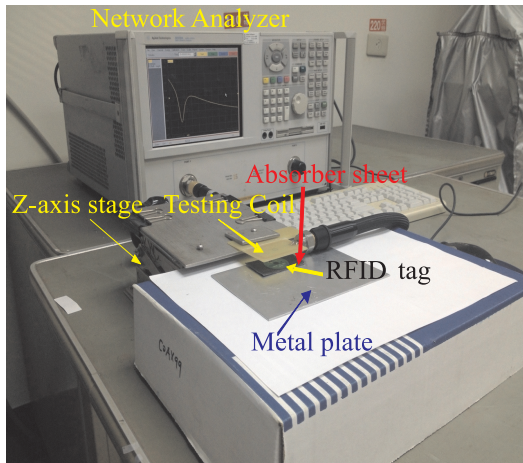


Fig.2. Measurement setup for measuring the reflection loss of antenna on the absorber sheet as substrate and metal plate.

communication was activated. For HF RFID application, the tag could perform best if the minimal reflection occurred around 13.56 MHz (the communication frequency for the now commercially-available HF RFID). In this work, Γ was measured by the terminated one-port technique using the S_{11} test fixture, therefore, $\Gamma = S_{11}$. The intensity and the frequency at the reflection loss minimum (f_r) depended on the properties and thickness of the absorber sheet. Besides, the mixture after 900°C calcinations was also pressed at a pressure 100 MPa to form a toroidal body (outer diameter of 9.5 mm, inner diameter of 3.8 and 5 mm height). The toroidal cores were sintered at 1050~1200°C for 1hr in air atmosphere to form spinel ferrite. The microstructure of the sintered specimens was investigated by a scanning electron microscopy (SEM). The density and magnetic properties, e.g., initial permeability (μ_i), of the sintered specimens were also measured.

3. RESULTS AND DISCUSSION

3.1. Properties of electromagnetic wave absorber

The electromagnetic wave absorption ability of the sintered NiCuZn ferrite absorber sheets as compared to a ferrite composite absorber sheet is shown in Fig.3. The absorber sheets designed with thickness of 0.1mm were prepared for the scaled-down RFID electronic components. The Γ , which corresponds to the electromagnetic wave absorption ability, of the sintering NiCuZn ferrites (C) are obviously larger than that of the ferrite composite ones (A, B) due to their higher initial permeability⁽⁷⁾. The frequency at the reflection loss minimum (f_r) of the sintering NiCuZn ferrites is closer to the commercially available 13.56 MHz RFID⁽⁸⁾.

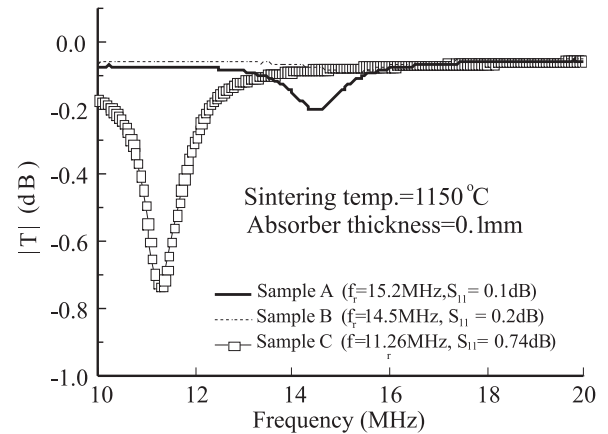


Fig.3. Electromagnetic wave reflection loss of ferrite composite absorber sheets (A, B) and the sintered NiCuZn ferrites absorber sheet (C).

3.2. Effect of sintering temperature

The electromagnetic wave absorption ability of the sample C sintered at 1050, 1100, 1150 and 1200°C are compared in Fig.4. The reflection loss of the absorber sheet is found to increase with increasing sintering temperature and achieves its maximum value at 1150°C. Besides, the minimum reflections of the absorber sheets, except that sintered at 1050°C, are all observed at a frequency of around 11.5 MHz.

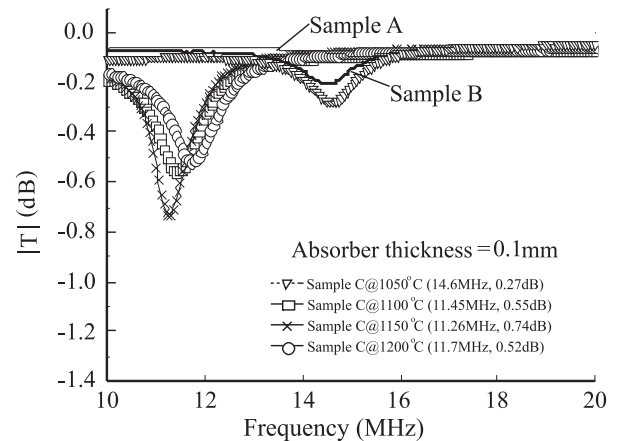


Fig.4. Electromagnetic wave absorption property of the sample C sintered at 1050, 1100, 1150 and 1200°C.

The DC resistivities (ρ_{dc}) of sample C sintered at 1050, 1100, 1150 and 1200°C are compared in Fig.5. The DC resistivity (ρ_{dc}) is also observed with different variations in the sintering temperature. The higher the sintering temperature, the larger the value of ρ_{dc} . The very low ρ_{dc} at 1050°C is due to defects and inhomogeneity inside the NiCuZn ferrite film that could not be repaired effectively at relatively low sintering temperatures⁽¹²⁾.

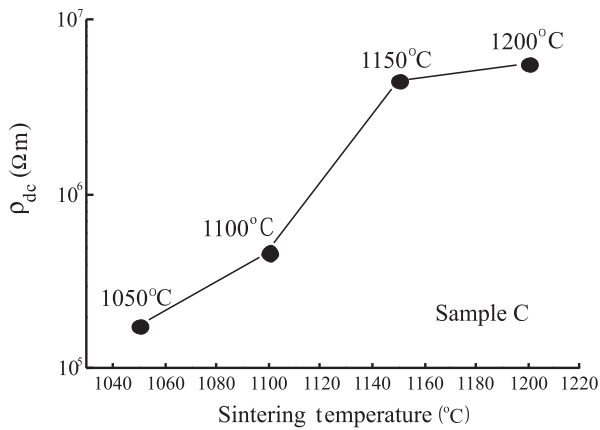


Fig.5. Sintering temperature versus ρ_{dc} .

The SEM micrograph ($\times 2K$) shown in Fig.6 revealed that the grain size of the sintered absorber sheets increases with increasing sintering temperature. A more homogenous microstructure in the sintered absorber sheet was obtained at 1150°C. The sintering temperature of the ferrite can lead to changes in grain size and the defect density, thus affecting the absorption properties depicted in Fig.4. Further, it may be noticed that intergranular pores were clearly observable in the

1200°C sintered absorber sheet shown in Fig.6(d). At very high sintering temperatures, however, such as those above 1200°C, porosity develops in the ferrite materials. This phenomenon could explain why the reflection loss decreased at an excessively high sintering temperature.

Figure 7 depicts the X-ray powder diffraction (XRD) patterns of NiCuZn ferrite (sample C) sintered at 1050, 1100, 1150 and 1200°C for 1 hr, respectively. The XRD patterns show a peak intensity as the crystalline phase is reached but the peak width decreased with the increasing sintering temperature, showing a clear decline at 1200°C. The sharper peaks indicate the more homogenous and better crystalline structure at higher sintering temperatures. However, the excessively high sintering temperature of 1200°C lowers the peak intensity, which could be related to the formation of a lot of intergranular pores, as shown in the SEM micrograph in Fig.6(d). The above phenomenon supports the finding that the best absorption ability is achieved at 1150°C sintering temperature, as depicted in Fig.4.

3.3. Material constants (μ, ϵ) and absorption characteristics

$\epsilon = \epsilon' - j\epsilon''$ is the complex relative dielectric permit-

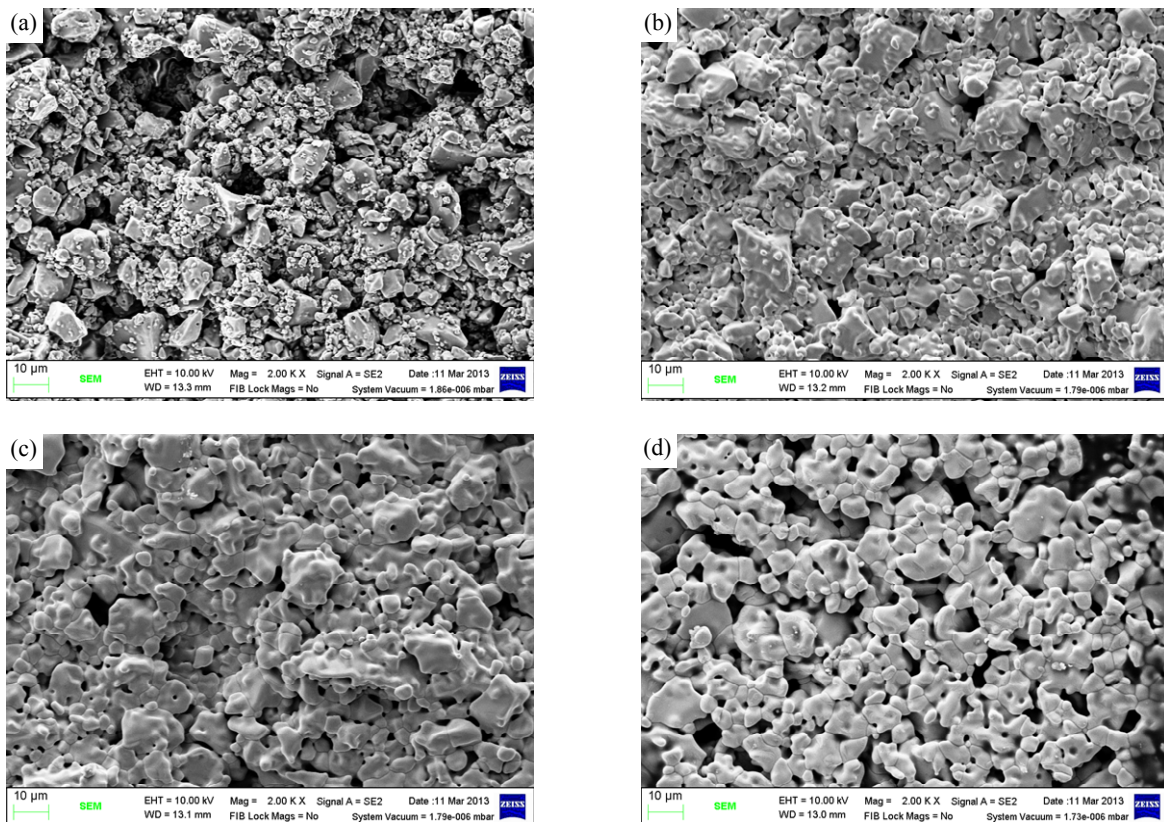


Fig.6. SEM micrograph ($\times 2K$) of sample C sintered at (a) 1050°C; (b) 1100°C; (c) 1150°C and (d) 1200°C.

tivity, with ϵ' being the real part or dielectric constant, and ϵ'' being the imaginary part or dielectric loss. $\mu = \mu' - j\mu''$ is the complex relative magnetic permeability, with μ' being the real magnetic permeability, and μ'' being the imaginary magnetic permeability or magnetic loss.

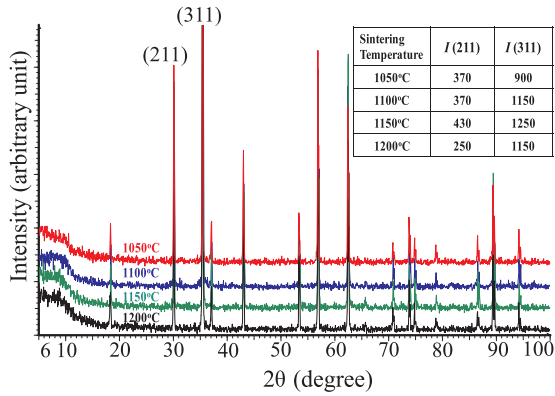


Fig. 7. X-ray powder diffraction pattern of NiCuZn ferrite sintered at 1050, 1100, 1150 and 1200°C for 1 hr, respectively.

Figure 8 shows the complex permeability (μ' , $-j\mu''$) and dielectric constant (ϵ' , $-j\epsilon''$) spectra observed in the sintering absorber sheets (Sample C) sintered at 1050, 1100, 1150, 1150°C, respectively. These data are measured by Agilent E4991A RF Impedance/Material Analyzer. The material constants μ' , μ'' , ϵ' and ϵ'' are the all increasing function of sintering temperature. ϵ' is a nearly constant value of about 1.5, and ϵ'' was found to be negligibly small. Obvious changes in μ' , μ'' , ϵ' and ϵ'' are perceived with variation of the sintering temperature. The higher the sintering temperature, the larger the resulting values of μ' , μ'' , ϵ' and ϵ'' . The larger μ'' and ϵ'' indicate the better absorption property of the absorber sheet^(10,11). The results in Figs.8(b) and (d) are in good agreement of the absorption properties shown in Fig.4. Moreover, the refractive index (n) of the absorber sheet is influential to the absorption property of absorber sheet^(10,11). The value of n is proportional to $(\epsilon\mu)^{1/2}$ of the absorber sheet. Based on the impedance matching theory, the wavelength of incident electromagnetic wave passing through a medium need to be smaller when the thickness of the medium is thinner⁽¹¹⁾.

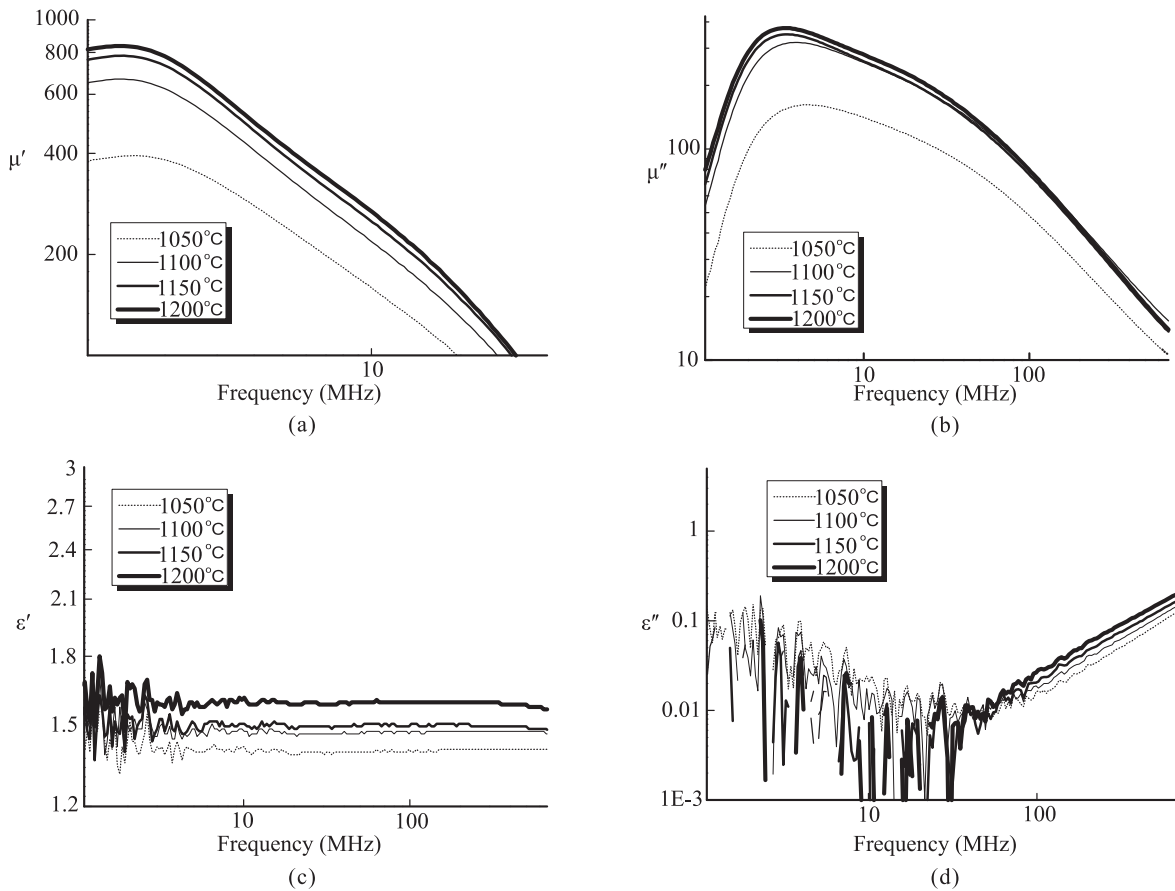


Fig. 8. Material constants versus frequency spectra measured in NiCuZn absorber sheet sintered at 1050, 1100, 1150 and 1200°C for 1 hr, respectively. (a) μ' ; (b) μ'' ; (c) ϵ' ; (d) ϵ'' .

Besides, if the absorber sheet has a larger refractive index, the wavelength of incident electromagnetic wave becomes smaller ($\lambda \propto n^{-1}$). Thus, there could be more incident electromagnetic wave entering the absorber sheet to make a higher probability of the absorption “occurring” in the absorber sheet^(11,12). The value of $(\epsilon\mu)^{1/2}$ of absorber sheet are shown in Fig.9, which reveals that the NiCuZn ferrite absorber sheet sintered at a higher temperature has a better absorption property (except for 1200°C due to pores induced at the unduly high temperature). From the above discussion, the sintering temperature at 1150°C should be appropriate for the NiCuZn ferrite selected in this study.

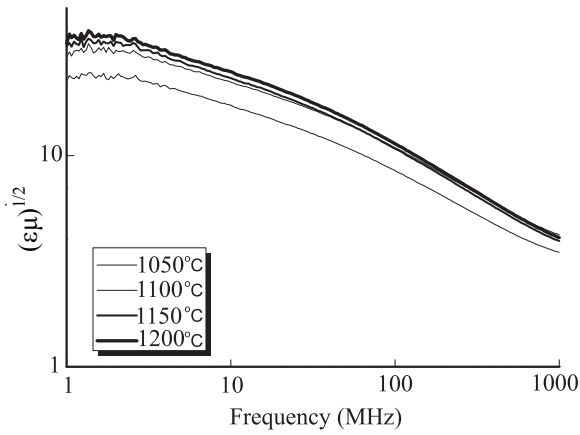


Fig.9. $(\epsilon\mu)^{1/2}$ versus frequency spectra measured in NiCuZn absorber sheet sintered at 1050, 1100, 1150 and 1200°C for 1 hr, respectively.

The inductance value (L) and the impedance value (Z) data are measured by an Agilent 4294A Precision Impedance Analyzer. The inductance measurements follow the measurement method⁽¹³⁾ and the JIS standard⁽¹⁴⁾. The inductance value (L) and impedance value (Z) of sample C sintered toroidal cores with 5 turns wound were measured as shown in Fig.10. Both of the value of L and Z are the decreasing functions of the results of minimum reflection loss frequency (f_r) shown in Fig.4. The above results could provide us a good reference to predict f_r of an absorber sheet; however, the mechanism between L , Z and f_r is not clear here.

4. CONCLUSIONS

Single and thin layer electromagnetic wave absorber sheets of 0.1 mm for use in the HF region were made by the simple technique of blade casting method with the addition of a proper selection of NiCuZn ferrites at the appropriate sintering temperature of 1150°C. The primary effect of the sintering

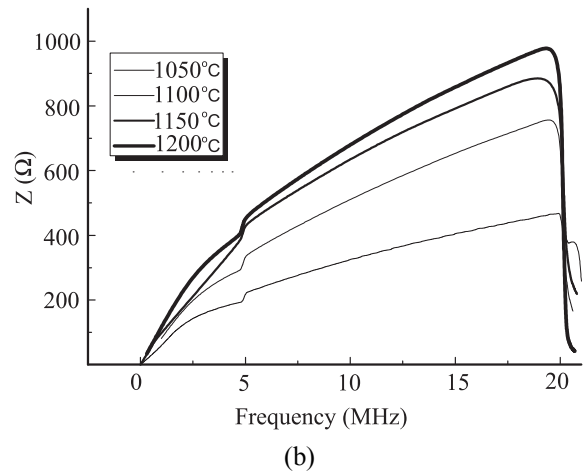
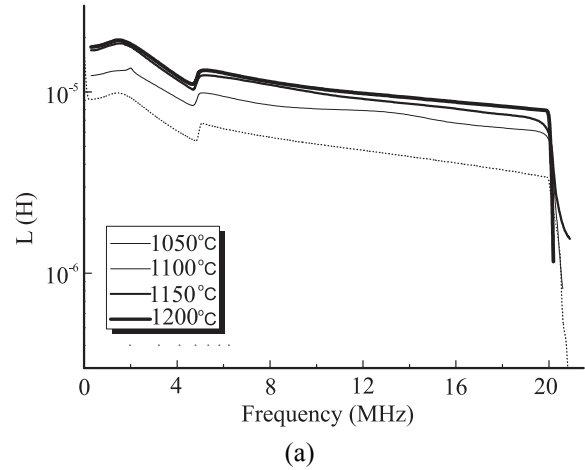


Fig.10. Measured frequency versus (a) Inductance value; and (b) Impedance value of sample D toroidal cores sintered at 1050, 1100, 1150 and 1200°C for 1 hr, respectively.

temperature was to increase the value of impedance value (Z) and inductance (L) of the sintered toroidal cores. Furthermore, the magnetic permeability (μ), the dielectric constant (ϵ) and the reflection loss (i.e., Γ , absorption property) of the absorber sheet are also enhanced at the higher sintering temperature. The more homogenous microstructure of the absorber sheets revealed in the SEM micrograph and the better crystalline XRD pattern could explain the best absorption ability at the 1150°C sintering temperature. The electromagnetic absorption characteristics were also successfully analyzed by taking into account that both the f_r shift correlated with L and Z of sintered toroidal cores and the electromagnetic wave absorption ability $|\Gamma|$ depended on ϵ'' , μ'' and $(\epsilon\mu)^{1/2}$. In this work, the results of high absorption ability ($|\Gamma| > 0.74$ dB) and wide-bandwidth (1.3 MHz) around 13.56 MHz indicates that sintered ferrite sheet could be used to effectively improve the coupling between RFID tags and readers and reduce destructive interference.

5. ACKNOWLEDGEMENTS

The authors would like to thank Mr. Sung-Jung Sung who has contributed to sample preparation and made experiment suggestions. Special thanks should also go to Dr. Chin-Lin Huang, Mr. Kuan-Jye Chen and Dr. Chien-Ming Lee for their strong support, as this work would not have been possible without them.

REFERENCES

1. J. Y. Hsu, S. K. Kuo and Y. H. Hung, "Electromagnetic properties of phosphate-coated ferrite composite materials", *J. Mater. Sci.: Mater. Electron.*, vol. 23 (2012), pp. 1944–1949.
2. H. M. Musal, Jr. and H. T. Hahn, "Thin-layer electromagnetic absorber design," *IEEE Trans. Magn.*, vol. MAG-25, No. 5 (May 1989), pp. 3851–3853.
3. A. N. Yusoff, M. H. Abdullah, S. H. Ahmad, S. F. Jusoh, A. A. Mansor and S. A. A. Hamid, "Electromagnetic and absorption properties of some microwave absorbers", *J. App. Phys.*, vol. 92, no. 2 (2002), pp. 876–882.
4. R. Dosoudil, M. Usakova, J. Franek, J. Slama and A. Gruskova, "Particle size and concentration effect on permeability and EM-wave absorption properties of hybrid ferrite polymer composites", *IEEE Trans. Magn.*, vol. 46 (2012), pp. 436–439.
5. J. Y. Hsu, W. S. Ko, H. D. Shen, and C. J. Chen, "Low temperature fired NiCuZn ferrite", *IEEE Trans. Magn.*, vol. 30 (1994), pp. 4875–4877.
6. Shih-Kang Kuo, Jen-Yung Hsu and Yung-Hsiung Hung, "A performance evaluation method for EMI sheet of metal mountable HF RFID tag", *Measurement*, vol. 44 (2011), pp. 946–953.
7. Jozef Slama, Peter Siroky, Martin Soka, Anna Gruskova and Vladimir Jancarik, "Frequency analysis of nickel based magnetic dielectrics", *Journal of Electrical Engineering*, vol. 60, no.1 (2009), pp. 39–42.
8. K. Finkenzerler, *RFID Handbook: Fundamentals and Applications in Contactless Smart Cards and Identification*, 2nd ed., New York, John Wiley & Sons, 2003.
9. Mrugesh Desai, Shiva Prasad, N. Venkataramani, Indradev Samajdar and A. K. Nigam, "Anomalous variation of coercivity with annealing in nanocrystalline NiZn ferrite films", *J. App. Phys.*, vol. 91, no. 10 (2002), pp. 7592–7594.
10. S. Gu, J. P. Barrett, T. H. Hand, B.-I. Popa and S. A. Cummer, "A broadband low-reflection metamaterial absorber", *J. App. Phys.*, vol. 108 (2010), 064913.
11. E. F. C. Driessen and M. J. A. de Dood, "The perfect absorber", *App. Phys. Lett.*, vol. 94 (2009), 171109.
12. P. Spinelli and A. Polman, "Prospects of near-field plasmonic absorption enhancement in semiconductor materials using embedded Ag nanoparticles", *Optics Express*, vol. 20, no. S5 (2012), pp. 641–654.
13. Solutions for Measuring Permittivity and Permeability with LCR Meters and Impedance Analyzers, Application Note 1369-1, Agilent, 2012, p. 17.
14. Japanese Industrial Standard (2006), Testing methods for water vapour permeability of textiles, JIS L, 1099. □